

LANGLEY GRANT

IN-64-CR

99100

45P

CONTROLLER DESIGN
via
STRUCTURAL REDUCED MODELING BY FETM

October 01, 1987

✓
Final Report
(Grant No. NAG-1-622)

Prepared for
NASA Langley Research Center,
Hampton, Virginia 23665

Submitted by

Drexel University
Department of Mechanical Engineering and Mechanics
Philadelphia, Pennsylvania 19104

{NASA-CR-180416} CONTROLLER DESIGN VIA
STRUCTURAL REDUCED MODELING BY FETM Final
Report (Drexel Univ.) 45 p Avail: NTIS
HC A03/MF A01

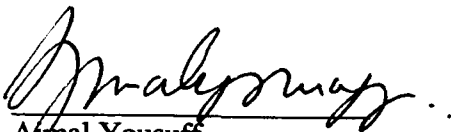
CSSL 12A

N87-30112

Unclass

G3/64 0099100

Principal Investigator:



Ahmad Yousuff
Assistant Professor
(215) 895-1868

Foreword

This annual report was prepared by the Department of Mechanical Engineering and Mechanics, Drexel University, Philadelphia, Pennsylvania 19104 under NASA Grant NAG-1-622. The work was performed under the direction of Dr. Jer-Nan Juang of the Structural Dynamics Branch of NASA Langley Research Center, Hampton, Virginia 23665.

The technical work was conducted by Dr. Ajmal Yousuff, Principal Investigator and the numerical work was performed by Mr. Mike Konstantinidis, graduate research assistant. This report covers the research performed during January 01, 1986 - July 31, 1987.

The investigator of this study wishes to thank Dr. Jer-Nan Juang for his guidance and support of this research, and his colleagues Dr. Leon Bahar and Dr. Tein-Min Tan for several discussions and assistance.

ABSTRACT

The Finite Element - Transfer Matrix (FETM) method has been developed to reduce the computations involved in analysis of structures. This widely accepted method, however, has certain limitations, and does not address the issues of control design. To overcome these, a modification of FETM method has been developed. The new method easily produces reduced models that are tailored toward subsequent control design. Other features of this method are its ability to (i) extract open loop frequencies and mode shapes with less computations, (ii) overcome limitations of the original FETM method, and (iii) simplify the design procedures for output feedback, constrained compensation, and decentralized control.

This report presents the development of the new method, generation of reduced models by this method, their properties, and the role of these reduced models in control design. Examples are included to illustrate the methodology.

TABLE OF CONTENTS

Foreword	ii
ABSTRACT	iii
I. INTRODUCTION.....	1
II. A NEW METHOD BASED ON FETM.....	3
2.1 Brief Review of FETM method.....	3
2.2 A New Method.....	6
2.2.1 Development.....	6
2.2.2 Algorithm	9
2.2.3 Remarks on the Algorithm.....	10
2.2.4 Variations of the Algorithm	13
2.3 Example.....	17
III. APPLICATION TO CONTROL DESIGN.....	23
3.1 Development	24
3.2 Control Design.....	27
IV. CONCLUSIONS	35
REFERENCES.....	37
APPENDIX A.....	39
APPENDIX B.....	44

I. INTRODUCTION

The straightforward applications of the existing theories to control of flexible structures is hindered by the dimension of their mathematical models. The control engineers have attempted to resolve this problem by resorting to some model reduction scheme. The control system that is designed based upon this reduced model is known to cause the detrimental "spill over" problems due to model errors, in general*. On the general topic of model reduction, many schemes have been developed which attempt to minimize model errors of one form or another. In the field of flexible structures, in addition to the structural analysts' approach [2] whereby lower natural frequencies are retained, there is the truncation scheme based on performance sensitivity measures of the closed loop modes [3,4], modal cost analysis [5], and the residual flexibility procedure [6] which retains the static contributions of the deleted modes. With the exception of a few [3-5], all these schemes are based upon an invalid assumption that the modeling/model-reduction and the control design problems are separable. Once an attempt is made to integrate these two inseparable problems, it becomes evident that a good design philosophy can be generated only by employing the modeling techniques of structural analysts and the control theory of control engineers simultaneously. The need for control/structure interaction has been recognized as evidenced by special sessions in related conferences [7,8], and the first NASA/DOD Conference totally devoted to this subject [9]. Number of papers, in addition to Ref.[10], supporting this subject are contained in Ref.[11]. Such an integration of the two disciplines forms the basic objective of this research effort.

There exist several methods in computational structural mechanics that aid and improve the analysis and design of structures; Noor and Alturi offer a comprehensive survey of such methods in Ref.[12]. The methods that are of interest to the current investigation are those which produce lower order models; control engineers need these lower order models in order to overcome the "dimension problem" mentioned above. A method that seems to be well suited for this task is the finite element transfer matrix (FETM) method [13-20]. The FETM method has been developed to overcome the problem of large size matrices that are encountered while modeling flexible structures within acceptable accuracy. The main advantage of the FETM method is that it yields a reduced set of equations by operating at the (finite-) elemental level. The advantages offered by the FETM method are not fully utilized in the area of control design. This is since the FETM method has been developed primarily for the open loop analysis by structural analysts and has not yet reached the control community.

* It has been pointed out in Ref.[1] that this may not always be the case.

The current research effort is an attempt to advance the FETM method, along with necessary modifications, to the control community as a viable tool for integrating structural modeling and control design phases. With a brief review of the FETM method and its limitations, Chapter II presents a new method that overcomes the limitations of the FETM method. Chapter II deals only with the extraction of natural frequencies and mode shapes. Chapter III discusses the possible role of this new method in control design with some illustrative examples. The report is concluded in Chapter IV with recommendations and directions for future research.

II. A NEW METHOD BASED ON FETM

The finite element technique is the most versatile tool in analyzing dynamic response problems of complex structures, particularly in evaluating natural frequencies and mode shapes. In order to describe a structure with good accuracy, it is necessary to divide the structure into a very large number of elements which in turn necessitates a large number of degrees of freedom (dof). This leads to large mass and stiffness matrices requiring significant amount of computer time to process. Consequently, alternative methods for reduction of the number of dof associated with a given structure have been developed. One of the most effective methods of order reduction which appears to be compatible with active control is the finite element transfer matrix (FETM) method [13].

The transfer matrix method is based on the selection of a state vector which is transmitted across the structure upon multiplication by a transfer matrix - the state vector consists of the dof and the generalized nodal forces along a section. Realizing that the number of dof in a finite element analysis of a structure can be considerably reduced by combining with the transfer matrix approach (which is most efficient when it is used along a dominant direction of a 'chain-like' structure), Dokainish [13] was the first to develop a combined method which exploited the best features of both the methods. He was able to show that the FETM method led to a frequency determinant of size 18 by 18, while the standard finite element technique produced a 108 by 108 determinant, the number of nodes being the same in both cases. The main advantage of the FETM method is that it yields a reduced set of equations by operating at the elemental level.

There are two limitations of the FETM method of Dokainish : (1) the method is applicable only to 'chain like' structures (these include beams and rectangular plates, but not circular plates), and (2) it requires the number of dof along the edges of all substructures to be the same. Several authors [14-20] have proposed means to overcome the second limitation by incorporating certain approximations. In these modified methods, though the second limitation of the FETM method is reduced, it is not completely eliminated. In what follows, we briefly discuss the FETM method of Dokainish, and present our new method, and conclude this chapter with an example.

2.1 Brief Review of FETM method

The transfer matrix method is generally associated with the concept of stiffness. Pestel and Lechie [21] demonstrated that for one-dimensional structural members such as

beams, the transfer matrix could be derived from the stiffness matrix. Dokainish [13] was the first to suggest a combined FETM method. He recognized that the transfer matrix method could be extended to two-dimensional chain like structures by deriving the transfer matrix for a plate strip from the corresponding stiffness matrix. Since the publication of Dokainish's paper, several authors (notably [14-20]) have proposed refinements and extensions of the FETM method. All of these authors derive the transfer matrix from the stiffness matrix in much the same fashion as Dokainish. This derivation, following that of Ref.[20], is summarized below.

The equation of motion of a structure can be written using a dynamic stiffness matrix S_e as

$$S_e q_e = f ; \quad S_e \triangleq K_e - \omega^2 M_e ; \quad (2.1)$$

where K_e is the stiffness matrix, M_e is the mass matrix, and ω is a natural frequency of the structure. Here q_e are the nodal displacements and f are the nodal forces. The standard finite element technique extracts the natural frequency ω by setting $|S| = 0$, where S is a submatrix of S_e , obtained after enforcing the boundary conditions that require some of the dof to be zero. Note that the size of this determinant is as large as the number of the total free dof used to describe the structure.

Consider now a structure which consists of N substructures. The dynamic stiffness equations of each structure can be obtained as in Eqn.(2.1) by employing finite element techniques. These equations for the i th substructure can be partitioned as

$$\begin{bmatrix} S_l^i & S_r^i \\ S_n^i & S_r^i \end{bmatrix} \begin{bmatrix} q_l^i \\ q_r^i \end{bmatrix} = \begin{bmatrix} f_l^i \\ f_r^i \end{bmatrix} \quad (2.2)$$

where f denotes the internal generalized forces; the subscripts 'l' and 'r' refer to quantities on the left and right boundaries of the substructure. Note the single subscripts on the diagonal submatrices S_l^i and S_r^i . In writing Eqn.(2.2) we have assumed that either there are no interior

nodes or the interior nodal displacements have been eliminated as mentioned in Ref.[21]. The transfer matrix T^i for the i th substructure is then found by manipulating Eqn.(2.2) to yield

$$\begin{bmatrix} -[S_l^i]^{-1} S_l^i & [S_l^i]^{-1} \\ -S_n^i + S_r^i [S_l^i]^{-1} S_l^i & -S_r^i [S_l^i]^{-1} \end{bmatrix} \begin{bmatrix} q_l^i \\ f_l^i \end{bmatrix} = \begin{bmatrix} q_r^i \\ -f_r^i \end{bmatrix} \quad (2.3a)$$

or simply

$$T^i x_1^i = x_r^i . \quad (2.3b)$$

Note the definition of the state vector x_r^i at the right boundary. Now for the adjacent (i+1)th substructure, equilibrium and continuity of displacements require that

$$x_1^{i+1} = x_r^i . \quad (2.4)$$

Equations (2.3b) and (2.4) are then combined to give

$$x_r^{i+1} = T^{i+1} T^i x_1^i . \quad (2.5)$$

Extending Eqn.(2.5) to N substructures results in

$$x_r^N = T x_1^1 ; \quad T \triangleq T^N T^{N-1} \dots T^1 , \quad (2.6)$$

where x_r^N and x_1^1 are the state vectors on the extreme right and left boundaries of the entire structure. Enforcing appropriate boundary conditions on x_r^N and x_1^1 would require $|T_f| = 0$ for a nontrivial response, where T_f is a submatrix of T . This condition is then used to extract the natural frequencies of the structure. Note that the size of this determinant is equal to the number of dof along a boundary.

The derivation of the transfer matrix from the dynamic stiffness matrix requires the inversion of the submatrix S_{rr}^i as shown in Eqn.(2.3a). In a strict sense, this inversion is possible if and only if S_{rr}^i is a square nonsingular matrix. However, S_{rr}^i is square if and only if there is an equal number of nodes (actual dof) on the right and left boundaries of the substructure, which in general may not hold. The submatrix S_{rr}^i , thus, cannot be inverted in general. Therefore, the above formulation of combined FETM method is only applicable to models which have the same number of dof on all substructure boundaries.

Recognizing that rectangular transfer matrices could occur in practice, Pestel [19] proposes using a left-inverse of S_{rr}^i . This is possible only if the number of nodes on the left boundary of a substructure is equal to or greater than that on the right boundary. This restricts Pestel's approach to structural models in which the number of nodes on the substructure boundaries decreases (or increases) monotonically from one exterior boundary to other. As suggested by Degen, *et al.* [20], a further extension of Pestel's procedure to rectangular transfer matrices would be to use a generalized-inverse, rather than a left-inverse, of S_{rr}^i . This however introduces approximations into the derivation of the transfer matrices from the stiffness matrices. More recent developments to overcome these limitations have

been reported by Degen, *et al.* [20], employing a mixed finite element formulation. In [20], the energy expression is obtained as Reissner functional, which allows the governing equations to be obtained in mixed form, that is, as a combination of stresses and displacements. This formulation permits the boundaries of a substructure to have a different number of dof "within certain limits"; the limits being that the number of nodes on the right boundary be not "too large" relative to the number on the left boundary. Hence, the limitation of the original FETM method, though reduced, are not completely eliminated.

2.2 A New Method

In this section, we present a new method, which completely eliminates the above limitations, without introducing any approximations. The development of this method is based on the fact that the natural frequency of a structure must render $|S| = 0$, where S is the dynamic stiffness matrix of the total structural model that results after enforcing the boundary conditions. That is, for an arbitrary partitioning of S , the natural frequency must satisfy

$$\begin{vmatrix} S_1 & S_{12} \\ S_{21} & S_2 \end{vmatrix} = 0, \quad (2.7a)$$

which, under the assumption of nonsingular S_1 yields

$$\begin{vmatrix} S_2 - S_{21}S_1^{-1}S_{12} \end{vmatrix} = 0. \quad (2.7b)$$

In what follows, we obtain Eqn.(2.7b) from operating at substructure level, instead of beginning with Eqn.(2.7a) which in general is of large dimension.

2.2.1 Development

Consider Eqn.(2.2), which is rewritten below for convenience

$$\begin{bmatrix} S_l^i & S_r^i \\ S_l^i & S_r^i \end{bmatrix} \begin{bmatrix} q_l^i \\ q_r^i \end{bmatrix} = \begin{bmatrix} f_l^i \\ f_r^i \end{bmatrix} ; \quad S_r^i = [S_r^i]^T \quad (2.8)$$

where q represents the 'free' dof (i.e., after enforcing the boundary conditions) on the left and right edges of the substructure as indicated by the subscripts 'l' and 'r' respectively. Using the top part of Eqn.(2.8),

$$S_{1,l}^i q_l^i + S_{r,l}^i q_r^i = F_{1,l}^{i,i} f_1^i \quad ; \quad F_{1,l}^{i,i} \triangleq I, \quad (2.9)$$

the q_l^i dof can be eliminated to obtain a reduced representation of the i th substructure in terms of only q_r^i :

$$S_{r,l}^{i,i} q_r^i = f_r^i + F_{r,l}^{i,i} f_1^i \quad (2.10a)$$

where,

$$S_{r,l}^{i,i} = [S_{r,l}^{i,i}]^T \triangleq S_r^i - S_{rl}^i [S_{1,l}^{i,i}]^{-1} S_{lr}^i \quad ; \quad S_{1,l}^{i,i} \triangleq S_1^i, \quad (2.10b)$$

$$F_{r,l}^{i,i} \triangleq - S_{rl}^i [S_{1,l}^{i,i}]^{-1} F_{1,l}^{i,i} \quad (2.10c)$$

Note that the inverse involved in Eqns.(2.10b,c) is only of a square symmetric matrix; we assume the existence of the inverse*. The ',' in the subscripts and superscripts are used to indicate that the corresponding elements (S and F in Eqns.(2.10a,b,c)) include some 'transferred' information - the information transferred is indicated by the subscripts and superscripts following the ','.

Now consider the dynamic stiffness matrix of the $(i+1)$ th substructure:

$$\begin{bmatrix} S_1^{i+1} & S_{lr}^{i+1} \\ S_{rl}^{i+1} & S_r^{i+1} \end{bmatrix} \begin{bmatrix} q_l^{i+1} \\ q_r^{i+1} \end{bmatrix} = \begin{bmatrix} f_1^{i+1} \\ f_r^{i+1} \end{bmatrix} \quad (2.11)$$

Under the assumption that there are no external forces present along the edge common to the i th and the $(i+1)$ th substructures, using Eqn.(2.10a) and the equilibrium condition

$$f_1^{i+1} + f_r^i = 0, \quad (2.12)$$

renders the top part of Eqn.(2.11) as

$$S_1^{i+1} q_l^{i+1} + S_{lr}^{i+1} q_r^{i+1} = F_{r,l}^{i,i} f_1^i - S_{r,l}^{i,i} q_r^i \quad (2.13)$$

In view of the continuity condition

$$q_l^{i+1} = q_r^i, \quad (2.14)$$

Eqn.(2.13) becomes

$$S_{1,l}^{i+1,i} q_l^{i+1} + S_{lr}^{i+1} q_r^{i+1} = F_{1,l}^{i+1,i} f_1^i, \quad (2.15a)$$

where, using the notation introduced in Eqns.(2.10b,c),

* The significance of this assumption will be discussed later in Section 2.2.2.

$$S_{l,l}^{i+1,i} = [S_{l,l}^{i+1,i}]^T \triangleq S_l^{i+1} + S_{r,l}^{i,i}, \quad (2.15b)$$

$$F_{l,l}^{i+1,i} \triangleq F_{r,l}^{i,i}. \quad (2.15c)$$

Note that, Eqn.(2.15a) is similar to Eqn.(2.9). Therefore, one can proceed as before to eliminate q_l^{i+1} from Eqn.(2.11). This yields a reduced representation of the i th and $(i+1)$ th substructures in terms of only q_r^{i+1} :

$$S_{r,l}^{i+1,i} q_r^{i+1} = f_r^{i+1} + F_{r,l}^{i+1,i} f_l^i, \quad (2.16a)$$

where,

$$S_{r,l}^{i+1,i} = [S_{r,l}^{i+1,i}]^T \triangleq S_r^{i+1} - S_{rl}^{i+1} [S_{l,l}^{i+1,i}]^{-1} S_{lr}^{i+1}, \quad (2.16b)$$

$$F_{r,l}^{i+1,i} \triangleq -S_{rl}^{i+1} [S_{l,l}^{i+1,i}]^{-1} F_{l,l}^{i+1,i}. \quad (2.16c)$$

Proceeding similarly, a reduced representation of the substructures $i, i+1, i+2, \dots, j$ ($j \geq i$), in terms of only q_r^j can be obtained as

$$S_{r,l}^{j,i} q_r^j = f_r^j + F_{r,l}^{j,i} f_l^i, \quad (2.17a)$$

where, for $k = i, i+1, \dots, j-1, j$,

$$\begin{aligned} S_{r,l}^{k,i} &= [S_{r,l}^{k,i}]^T \triangleq S_r^k - S_{rl}^k [S_{l,l}^{k,i}]^{-1} S_{lr}^k \\ S_{l,l}^{k,i} &= [S_{l,l}^{k,i}]^T \triangleq S_l^k + S_{r,l}^{k-1,i} \quad ; \quad S_{r,l}^{i-1,i} \triangleq 0 \\ F_{r,l}^{k,i} &= -S_{rl}^k [S_{l,l}^{k,i}]^{-1} F_{l,l}^{k,i} \end{aligned} \quad (2.17b)$$

$$F_{r,l}^{k,i} = -S_{rl}^k [S_{l,l}^{k,i}]^{-1} F_{l,l}^{k,i}$$

$$F_{l,l}^{k,i} = \begin{cases} F_{r,l}^{k-1,i} & ; \quad k > i \\ I & ; \quad k = i \end{cases}$$

We emphasize that the matrix inversions needed in Eqn.(2.17b) are only of square matrices. Hence, as long as these matrices are nonsingular, Eqn.(2.17a) can be obtained without introducing any approximations. Moreover, no assumptions have been made regarding the number of dof on the left and right edges of the substructures - the boundary

conditions of the substructures can be arbitrary. Thus, the second limitation of Dokainish's FETM method is totally eliminated. Means of overcoming the first limitation is described in Section 2.2.3.

2.2.2 Algorithm

We illustrate the use of Eqn.(2.17) in determining a natural frequency (ω) of a structure that is divided into N substructures - the substructures are numbered from left to right. It is assumed that the mass and stiffness matrices are available for all the substructures, hence, the elemental dynamic stiffness matrices can be calculated. We propose the following algorithm.

Determination of natural frequency

Step 0. Assume an initial value for ω .

Step 1. Set

$$S_{r,1}^{0,1} = 0; \quad k = 1$$

Step 2.

a) Calculate

$$S_{l,1}^{k,1} = S_l^k + S_{r,1}^{k-1,1} \quad (2.18a)$$

$$S_{r,1}^{k,1} = S_r^k - S_{rl}^k [S_{l,1}^{k,1}]^{-1} S_{lr}^k \quad (2.18b)$$

b) If $k = N$, go to *Step 3*.

If $k < N$, set $k = k + 1$, and repeat *Step 2*.

Step 3.

a) Determine

$$\Delta(\omega) \triangleq \left| S_{r,1}^{N,1} \right|. \quad (2.19)$$

b) If $|\Delta(\omega)| \leq \epsilon$, a prespecified representation of numerical zero, stop. The value of ω is a natural frequency of the structure.

If not, use an "appropriate" value for ω and go to *Step 1*.

The justification of this algorithm is based on the following theorem.

Theorem 2.1

Under the assumption of nonsingular $S_{l,l}^{k,1}$ for $1 \leq k \leq N$, the natural frequency ω of the structure satisfies $\Delta(\omega) = 0$.

Proof: Let $N = 1$. Then ω satisfies

$$\begin{vmatrix} S_1^1 & S_r^1 \\ S_{rl}^1 & S_r^1 \end{vmatrix} = |S_1^1| |S_{r,l}^{1,1}| = 0. \quad (2.20)$$

Since $S_1^1 = S_{l,l}^{1,1}$ is assumed to be nonsingular, Eqn.(2.20) results in, for $N = 1$,

$$\Delta(\omega) = |S_{r,l}^{N,1}| = 0. \quad (2.21)$$

Now let $N = 2$. Then ω must satisfy

$$\begin{vmatrix} S_1^1 & S_r^1 & 0 \\ S_{rl}^1 & S_r^1 + S_1^2 & S_r^2 \\ 0 & S_{rl}^2 & S_r^2 \end{vmatrix} = |S_1^1| \begin{vmatrix} S_1^2 + S_{l,l}^{1,1} & S_r^2 \\ S_{rl}^2 & S_r^2 \end{vmatrix} = |S_1^1| |S_{l,l}^{2,1}| |S_{r,l}^{2,1}| = 0,$$

which again yields Eqn.(2.21) for $N = 2$, under the assumption of nonsingular S_1^1 and $S_{l,l}^{2,1}$.

Proceeding similarly for a general N proves the theorem. #

2.2.3 Remarks on the Algorithm

A few remarks pertaining to this algorithm are in order.

a) The nonsingularity assumption of $S_{l,l}^{k,1}$

For the above algorithm to work it is necessary for $S_{l,l}^{k,1}$ ($1 \leq k \leq N$) to be nonsingular - an assumption made in the development of the algorithm. The significance of this assumption follows. Define

$$\delta_k(\omega) \triangleq |S_{l,l}^{k,1}|. \quad (2.22)$$

Then $S_{l,l}^{k,1}$ is singular if and only if $\delta_k(\omega) = 0$. Let $k = 1$. Then

$$\delta_1(\omega) = \left| S_{l,l}^{1,1} \right| = \left| S_1^1 \right|, \quad (2.23)$$

where S_1^1 is the dynamic stiffness matrix of the first substructure with its right edge fixed, i.e., $q_r^1 = 0$. Therefore, $\delta_1(\omega) = 0$ implies that the assumed frequency is a natural frequency of the first substructure with its right edge fixed. Hence, the nonsingularity assumption of $S_{l,l}^{1,1}$ only implies that the assumed value of ω is not one of the frequencies of the first substructure with its right edge fixed. We shall assume this is the case, and let $k = 2$. Then

$$\begin{aligned} \delta_2(\omega) &= \left| S_{l,l}^{2,1} \right| = \left| S_1^2 + S_{r,l}^{1,1} \right| = \left| S_1^2 + S_r^1 - S_{rl}^1 [S_{l,l}^{1,1}]^{-1} S_{lr}^1 \right| \\ &= \frac{1}{\delta_1(\omega)} \left| \begin{array}{cc} S_{l,l}^{1,1} & S_{lr}^1 \\ S_{rl}^1 & S_r^1 + S_1^2 \end{array} \right|. \end{aligned} \quad (2.24a)$$

Consider now a structure that consists of only the first and second substructures with the right end of the second substructure being fixed, i.e., $q_r^2 = 0$. Then the natural frequency of this structure must satisfy

$$\left| \begin{array}{cc} S_l^1 & S_{lr}^1 \\ S_{rl}^1 & S_r^1 + S_1^2 \end{array} \right| = \delta_1(\omega) \delta_2(\omega) = 0. \quad (2.24b)$$

Therefore, comparison of Eqns.(2.25a) and (2.25b) reveals that $\delta_2(\omega) = 0$ if ω is a natural frequency of this "2-element" structure whose right edge is fixed. Proceeding similarly, we arrive at the conclusion that the nonsingularity assumption of $S_{l,l}^{k,1}$ is violated if the assumed value of ω is one of the frequencies of a structure that consists of only k substructures with its right edge fixed.

b) The choice of an "appropriate" ω

Note that in *Step.3b* there is a need for an appropriate updating of ω . Currently, we are using a variation of the successive bisection method to update ω , and it seems to work efficiently for the beam examples considered herein. There may exist other methods that work more efficiently. An appropriate method needed in *Step.3b* is under investigation.

c) *Inclusion of spring-support/point-mass*

The presence of any spring-support and/or concentrated point masses at any of the intermediate nodes of the structure can be easily accommodated in this algorithm. This can be achieved as follows. Suppose that some nodes along the edge common to i th and $(i+1)$ th substructures have spring supports and/or point masses. Then, to take these into account, the equilibrium condition Eqn.(2.12) must be expressed as

$$\mathbf{f}_l^{i+1} + \mathbf{f}_r^i = [\mathbf{K}_{i+1}^i - \omega^2 \mathbf{M}_{i+1}^i] \mathbf{q}_l^{i+1} \quad (2.25a)$$

where \mathbf{K}_{i+1}^i (resp. \mathbf{M}_{i+1}^i) is a diagonal matrix consisting of the spring constants of the spring supports (resp. masses of the point masses) - some of these may be zeros along its diagonal. Then, the dynamic stiffness matrix $\mathbf{S}_{l,l}^{i+1,j}$ would correspondingly change to

$$\mathbf{S}_{l,l}^{i+1,j} = \mathbf{S}_l^{i+1} + \mathbf{S}_{r,l}^{i+1,j} + [\mathbf{K}_{i+1}^i - \omega^2 \mathbf{M}_{i+1}^i]. \quad (2.25b)$$

The presence of spring-support and/or point-masses along the left and right boundaries of the overall structure can be similarly taken into account.

d) *Determination of Mode Shapes*

In the absence of any external forces, Eqn.(2.17a), for $j = N$ and $i = 1$ yields

$$\mathbf{S}_{r,l}^{N,1} \mathbf{q}_r^N = 0, \quad (2.26)$$

from which, in view of $\Delta(\omega) = 0$, a nontrivial \mathbf{q}_r^N can be determined. Then using the equation, analogous to Eqn.(2.15a),

$$\mathbf{S}_{l,l}^{N,1} \mathbf{q}_l^N + \mathbf{S}_{lr}^N \mathbf{q}_r^N = 0 \quad (2.27)$$

$\mathbf{q}_l^N (= \mathbf{q}_r^{N-1})$ can be determined. Proceeding similarly, the entire mode shape of the structure, corresponding to that frequency, can be determined.

e) *Development from assembled equations.*

Note that the computations involved in *Step.2a* are repetitive, i.e., they are repeated for $k = 1, 2, \dots, N$, indicating that the computations are carried out at substructure level as one proceeds from the first ($k=1$) to the last ($k=N$) substructure via the intermediate substructures ($k=2, 3, \dots, N-1$). The final outcome of this step is the matrix $\mathbf{S}_{r,l}^{N,1}$. This matrix

can also be obtained from the complete assembled dynamic stiffness matrix S representing the total structure, though this involves inversion of larger matrices. This follows from the proof of Theorem 2.1.

2.2.4 Variations of the Algorithm

Variation A.

Note that the development, and the algorithm, assume that in obtaining Eqn.(2.19) one advances from left-to-right as the computations are performed at the substructures level. One could also advance from right-to-left to determine the natural frequency.

Determination of natural frequency: Variation A

Step 0. Assume an initial value for ω .

Step 1. Set

$$S_{l,r}^{N+1,N} = 0; \quad k = N$$

Step 2.

a) Calculate

$$S_{r,r}^{k,N} = S_r^k + S_{l,r}^{k+1,N} \quad (2.28a)$$

$$S_{l,r}^{k,N} = S_l^k - S_r^k [S_{r,r}^{k,N}]^{-1} S_{r,l}^k \quad (2.28b)$$

b) If $k = 1$, go to *Step 3*.

If $k > 1$, set $k = k - 1$, and repeat *Step 2*.

Step 3.

a) Determine

$$\Delta(\omega) \triangleq \left| S_{l,r}^{1,N} \right|. \quad (2.29)$$

b) If $|\Delta(\omega)| \leq \epsilon$, a prespecified representation of numerical zero, stop. The value of ω is a natural frequency of the structure.

If not, use an "appropriate" value for ω and go to *Step 1*.

This approach amounts to transferring all dof (q_r^k ; $k = N, N-1, \dots, 2$) to q_l^1 in order to obtain,

as in Eqn.(2.26), a reduced representation of the structure in terms of q_l^1 :

$$S_{l,r}^{1,N} q_l^1 = 0. \quad (2.30)$$

In fact, one can obtain such a representation of the structure in terms of any dof, q_r^i (or q_l^j) as follows:

Variation B.

Proceed from left-to-right to obtain

$$S_{r,l}^{i,1} q_r^i = f_r^i, \quad (2.31a)$$

and proceed from right-to-left to obtain

$$S_{l,r}^{i+1,N} q_l^{i+1} = f_l^{i+1}. \quad (2.31b)$$

Now, enforcing the equilibrium and continuity conditions yields

$$[S_{r,l}^{i,1} + S_{l,r}^{i+1,N}] q_l^{i+1} = 0 \quad (2.31c)$$

The Eqn.(2.19) will then be replaced by

$$\Delta(\omega) = \left| S_{r,l}^{i,1} + S_{l,r}^{i+1,N} \right|. \quad (2.31d)$$

This procedure is summarized below:

Determination of natural frequency: Variation B

Step 0. Assume an initial value for ω .

Phase I.

Step I.1. Set

$$S_{r,l}^{0,1} = 0; \quad k = 1$$

Step I.2.

a) Calculate

$$S_{l,l}^{k,1} = S_l^k + S_{r,l}^{k-1,1} \quad (2.32a)$$

$$S_{r,l}^{k,1} = S_r^k - S_{rl}^k [S_{l,l}^{k,1}]^{-1} S_{lr}^k \quad (2.32b)$$

b) If $k = i$, go to *Step 3*.

If $k < i$, set $k = k + 1$, and repeat *Step I.2*.

Phase II.

Step II.1. Set

$$S_{l,r}^{N+1,N} = 0; k = N$$

Step II.2.

a) Calculate

$$S_{r,r}^{k,N} = S_r^k + S_{l,r}^{k+1,N} \quad (2.33a)$$

$$S_{l,r}^{k,N} = S_l^k - S_r^k [S_{r,r}^{k,N}]^{-1} S_{r,l}^k \quad (2.33b)$$

b) If $k = i+1$, go to *Step 3*.

If $k > i+1$, set $k = k - 1$, and repeat *Step II.2*.

Step 3.

a) Determine

$$\Delta(\omega) = \left| S_{r,l}^{i,1} + S_{l,r}^{i+1,N} \right|. \quad (2.34)$$

b) If $|\Delta(\omega)| \leq \epsilon$, a prespecified representation of numerical zero, stop. The value of ω is a natural frequency of the structure.

If not, use an "appropriate" value for ω and go to *Step 1*.

Variation C.

Moreover, the algorithm for determining the natural frequency can also be obtained in terms of any combination of the dof. Suppose, for example, that we wish to develop this algorithm in terms q_l^i and q_r^j ($1 < i < j < N$). Then, we could proceed as follows. Proceed

from first substructure to i th substructure to obtain

$$S_{l,l}^{i,1} q_l^i + S_{r,l}^i q_r^i = 0. \quad (2.32)$$

Proceed from N th substructure to j th substructure to obtain

$$S_{r,r}^{j,N} q_r^j + S_{r,l}^j q_l^j = 0. \quad (2.33)$$

Now, to eliminate the intermediate dof, we begin with (for convenience) the dof common to i th and $(i+1)$ th substructures:

$$S_{rl}^i q_l^i + [S_r^i + S_l^{i+1}] q_r^i + S_{lr}^{i+1} q_r^{i+1} = 0, \quad (2.34a)$$

and compute

$$q_r^i = -[S_r^{i,i+1}]^{-1} \{ S_{rl}^i q_l^i + S_{lr}^{i+1} q_r^{i+1} \}, \quad (2.34b)$$

where

$$S_r^{i,i+1} \triangleq S_r^i + S_l^{i+1}. \quad (2.34c)$$

Substituting Eqn.(2.34c) in Eqn.(2.32) yields

$$[S_{ll}^{i+1} - S_{lr}^i (S_r^{i,i+1})^{-1} S_{rl}^i] q_l^i - S_{lr}^i (S_r^{i,i+1})^{-1} S_{lr}^{i+1} q_r^{i+1} = 0. \quad (2.35)$$

Now consider the equations for q_r^{i+1} from the (i+1)th substructure:

$$S_{rl}^{i+1} q_l^{i+1} + S_r^{i+1} q_r^{i+1} = f_r^{i+1}, \quad (2.36a)$$

which in view of Eqn.(2.34b) and since $q_l^{i+1} = q_r^i$, becomes

$$-S_{rl}^{i+1} (S_r^{i,i+1})^{-1} S_{rl}^i q_l^i + [S_r^{i+1} - S_{rl}^{i+1} (S_r^{i,i+1})^{-1} S_{lr}^{i+1}] q_r^{i+1} = f_r^{i+1}. \quad (2.36b)$$

Then, using the equilibrium condition, q_r^{i+1} can be expressed in terms of q_l^i and q_r^{i+2} , which expression can then be used to write Eqn.(2.35) in terms of q_l^i and q_r^{i+2} . Proceeding similarly the following equations can be developed:

$$\begin{bmatrix} S_{11} & S_{12} \\ S_{21} & S_{22} \end{bmatrix} \begin{bmatrix} q_l^i \\ q_r^j \end{bmatrix} = 0, \quad (2.37)$$

where S_{ij} are obtained through the above sequential calculations. Eqn.(2.37) can then be used to determine the natural frequency.

Even though we have offered the above development - from Eqn.(2.32) to Eqn.(2.37) - as a variation of the algorithm of Section 2.2.3, this algorithm, along with its variations A and B are really special cases of Variation C. We have chosen to offer Variation C last in order to make the development more comprehensible.

Observe that Variation C of the algorithm can be used for structures that are not chain-like, such as circular plates, thereby eliminating the second limitation of the Dokainish's method.

2.3 Example

A simply supported beam, with some minor variations, is employed in this section to illustrate the applicability of the new method proposed herein. The beam under consideration is shown in Fig.2.1 below.

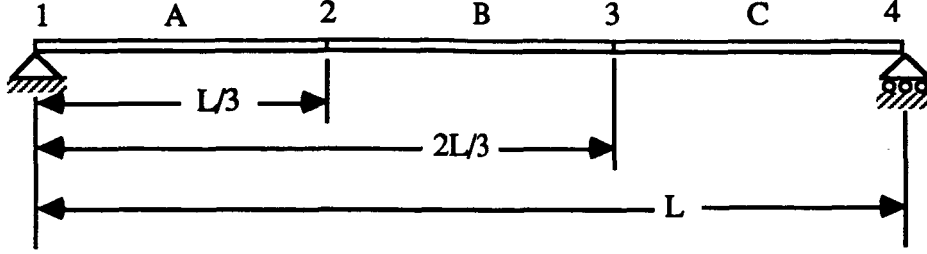


Fig. 2.1 Simply Supported Beam: 3 Elements

The beam is modeled by three (hence, $N = 3$) cubic beam finite elements A, B, and C with points 1, 2, 3, and 4 as the nodal points. The linear and the angular deflections of the beam are denoted by x and θ , respectively. The numerical value assumed for this beam are: the length of the beam $L = 1$; $\rho A = 420$, where ρ is the mass density per unit area, and A is the cross sectional area; $EI = 1$, where E is the modulus of elasticity, and I is the bending moment of inertia.

The following method illustrates the new method, as applied to this example.

The elemental mass and stiffness matrices are given below, with the elements numbered from left to right.

$$M^1 = \begin{bmatrix} 1.4815e-1 & -1.4444e+0 & -1.1111e-1 \\ -1.4444e+0 & 5.2000e+1 & 2.4444e+0 \\ -1.1111e-1 & 2.4444e+0 & 1.4815e-1 \end{bmatrix}; K^1 = \begin{bmatrix} 1.2000e+1 & 5.4000e+1 & 6.0000e+0 \\ 5.4000e+1 & 3.2400e+2 & 5.4000e+1 \\ 6.0000e+0 & 5.4000e+1 & 1.2000e+1 \end{bmatrix}$$

$$M^2 = \begin{bmatrix} 5.2000e+1 & -2.4444e+0 & 1.8000e+1 & 1.4444e+0 \\ -2.4444e+0 & 1.4815e-1 & -1.4444e+0 & -1.1111e-1 \\ 1.8000e+1 & -1.4444e+0 & 5.2000e+1 & 2.4444e+0 \\ 1.4444e+0 & -1.1111e-1 & 2.4444e+0 & 1.4815e-1 \end{bmatrix}$$

$$K^2 = \begin{bmatrix} 3.2400e+2 & -5.4000e+1 & -3.2400e+2 & -5.4000e+1 \\ -5.4000e+1 & 1.2000e+1 & 5.4000e+1 & 6.0000e+0 \\ -3.2400e+2 & 5.4000e+1 & 3.2400e+2 & 5.4000e+1 \\ -5.4000e+1 & 6.0000e+0 & 5.4000e+1 & 1.2000e+1 \end{bmatrix}$$

$$M^3 = \begin{bmatrix} 5.2000e+1 & -2.4444e+0 & 1.8000e+1 \\ -2.4444e+0 & 1.4815e-1 & -1.4444e+0 \\ 1.8000e+1 & -1.4444e+0 & 5.2000e+1 \end{bmatrix}; K^3 = \begin{bmatrix} 3.2400e+2 & -5.4000e+1 & -3.2400e+2 \\ -5.4000e+1 & 1.2000e+1 & 5.4000e+1 \\ -3.2400e+2 & 5.4000e+1 & 3.2400e+2 \end{bmatrix}$$

Hence, for the first element, the dynamic stiffness matrix is obtained as

$$S_1^1 = 1.2000e+1 - 1.4815e-1 * \omega^2$$

$$S_{lr}^1 = [S_h^1]^T = \begin{bmatrix} 5.4000e+1 + 1.4444e+0 * \omega^2 & 6.0000e+0 + 1.1111e-1 * \omega^2 \end{bmatrix}$$

$$S_r^1 = \begin{bmatrix} 3.2400e+2 - 5.2000e+1 * \omega^2 & 5.4000e+1 - 2.4444e+0 * \omega^2 \\ 5.4000e+1 - 2.4444e+0 * \omega^2 & 1.2000e+1 - 1.4815e-1 * \omega^2 \end{bmatrix}$$

Similarly the dynamic stiffness matrices for other elements can also be obtained. With these matrices available we are now in a position to use the algorithm of Section 2.2.2.

Using 0.48184 as the initial value for ω yields $\Delta(\omega) = 0.0047$. The variation of $\Delta(\omega)$ with ω is shown in Fig.2.2. The Table 2.1 gives the frequencies obtained by conventional finite element method and by the new method, and the value of $\Delta(\omega)$ corresponding to these values of the frequencies by the new method.

Table 2.1 Results for the system of Fig.2.1

ω by finite element	ω by new method	$\Delta(\omega)$
0.48184	0.48184	0.0047
1.94960	1.94960	0.0020
4.81120	4.81120	0.0043
8.94700	8.94470	0.0015
16.0110	16.0110	0.0021
22.0580	22.0580	0.0044

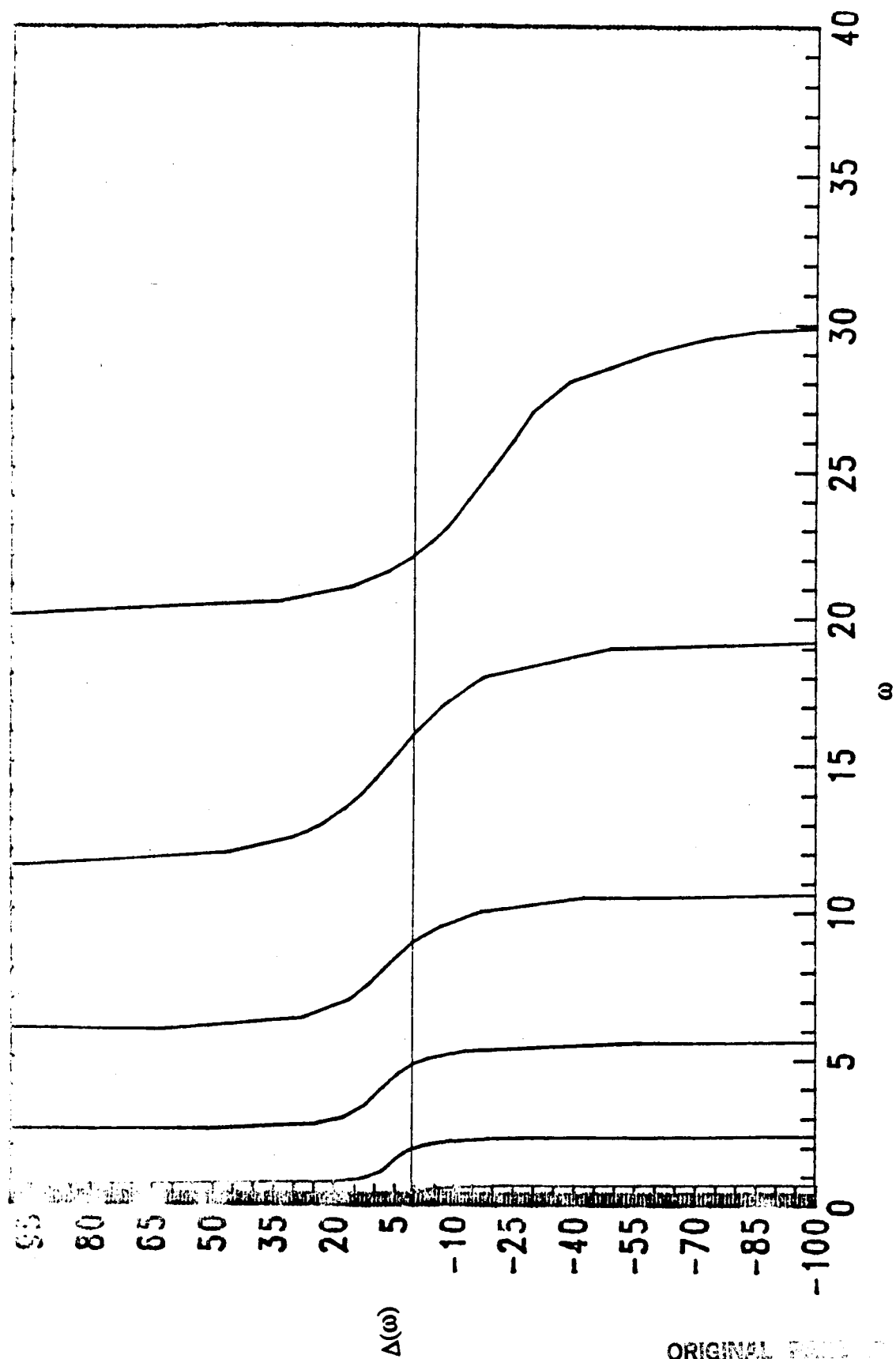


Fig.2.2. $\Delta(\omega)$ vs. ω for the system of Fig.2.1

ORIGINAL PAGE IS
OF POOR QUALITY

In the following few pages, we present the results obtained by employing the new method to different configurations of the simple beam. The numerical value used for the stiffness of the spring in Fig. 2.7 is 15 units. Note that the original FETM method can not applid to the configurations of Figures 2.5 and 2.7.

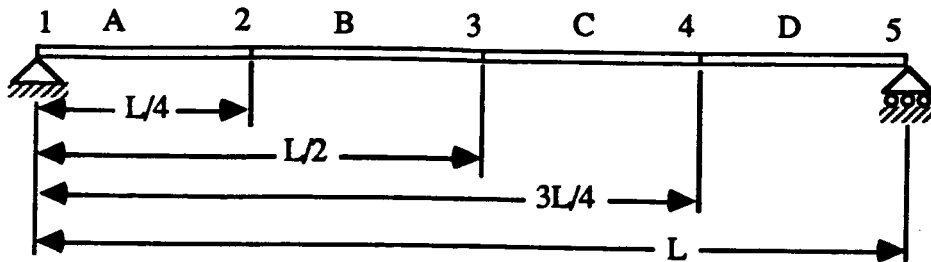


Fig. 2.3 Simply Supported Beam: 4 Elements

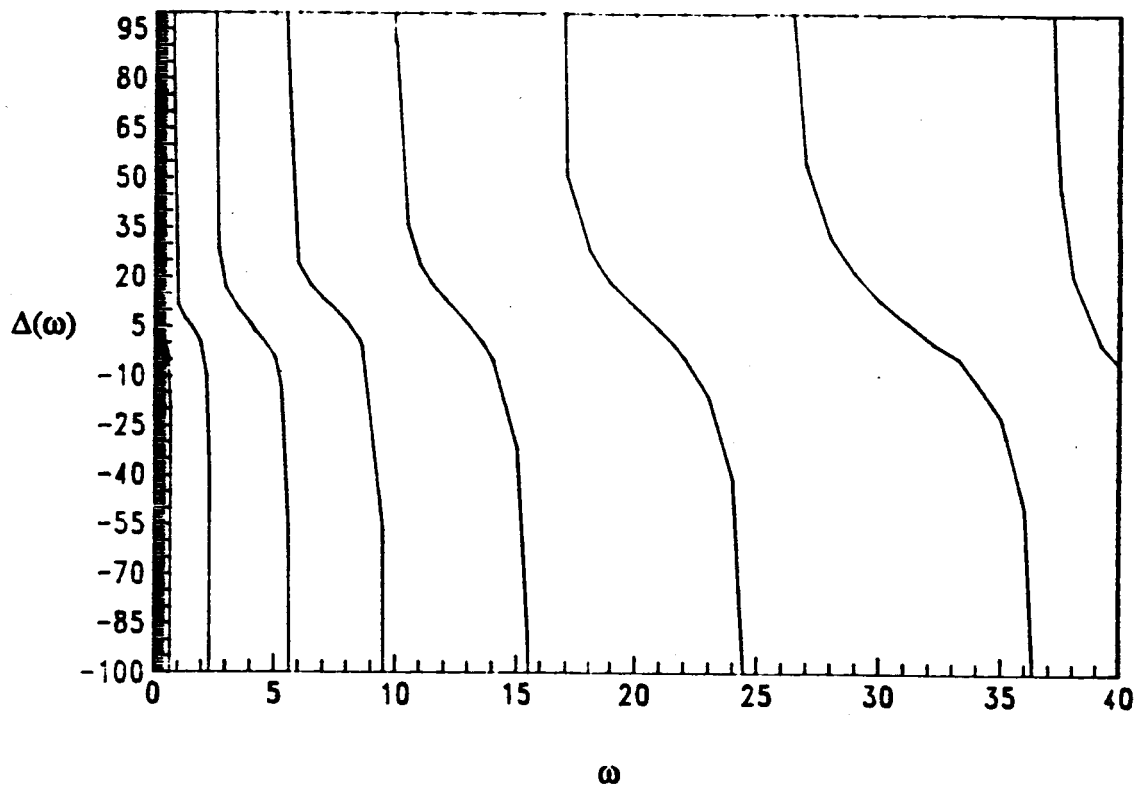


Fig.2.4. $\Delta(\omega)$.vs. ω for the system of Fig.2.3

Table 2.2 Results for the system of Fig.2.3

ω by finite element	ω by new method	$\Delta(\omega)$
0.48380	0.48380	0.0043
1.93430	1.93430	0.0070
4.41200	4.41250	0.0278
8.53690	8.53740	0.0214
13.5670	13.5900	0.0270
21.4970	21.4970	0.0004
31.9440	32.2200	0.0028
38.7870	39.2270	0.0040

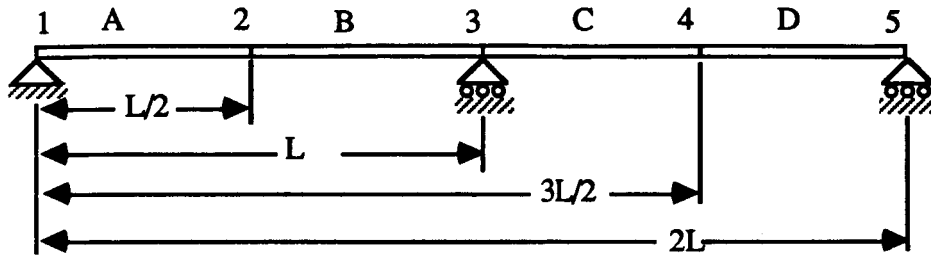


Fig. 2.5 Two span, simple beam

Table 2.3 Results for the system of Fig.2.5

ω by finite element	ω by new method	$\Delta(\omega)$
0.54309	0.54280	0.0500
0.87665	0.87600	0.0240
2.22700	2.22560	3.7967
3.13510	3.12350	-0.6428
5.70690	5.70870	0.0270
8.25750	8.25876	0.0004
10.3830	10.5223	0.0028

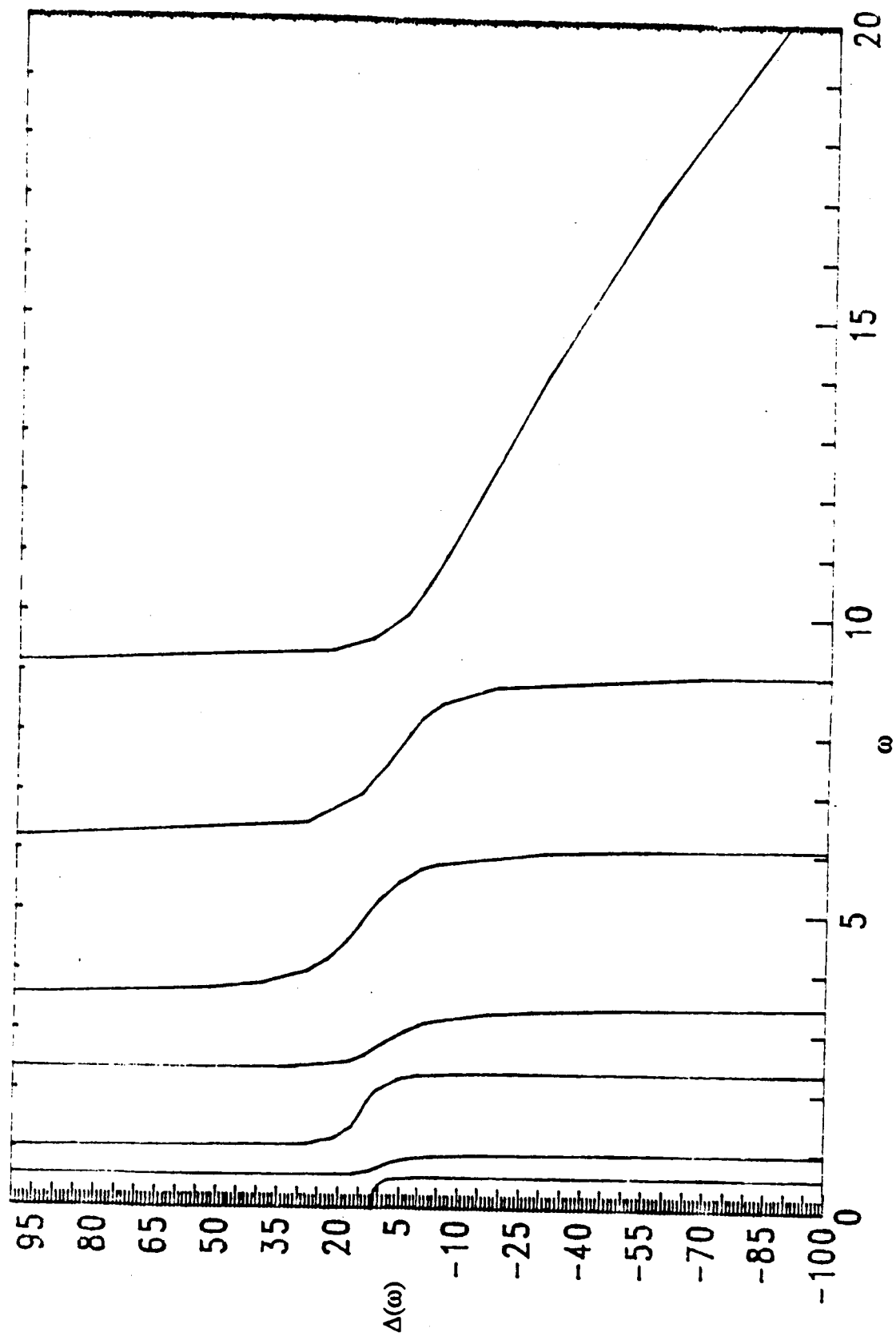


Fig.2.6. $\Delta(\omega)$ vs. ω for the system of Fig.2.5

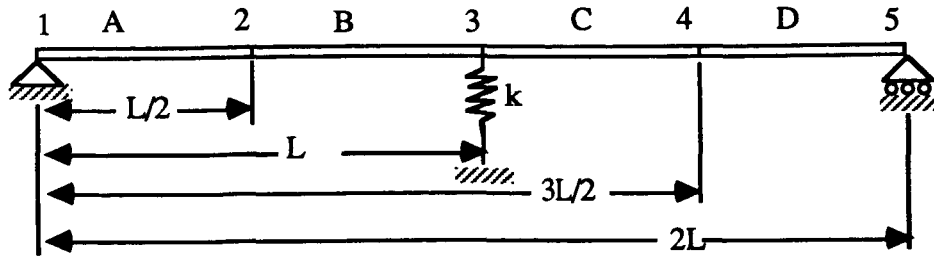


Fig. 2.7 spring supported, simple beam

Table 2.4 Results for the system of Fig.2.7

ω by finite element	ω by new method	$\Delta(\omega)$
0.17611	0.22100	0.0012
0.47222	0.48600	0.0097
1.13360	1.12100	0.0324
2.13720	2.13760	0.0257
3.40080	3.40400	0.0343
5.37510	5.37510	0.0026
8.05350	8.05350	0.0233
9.79780	9.79780	0.0421

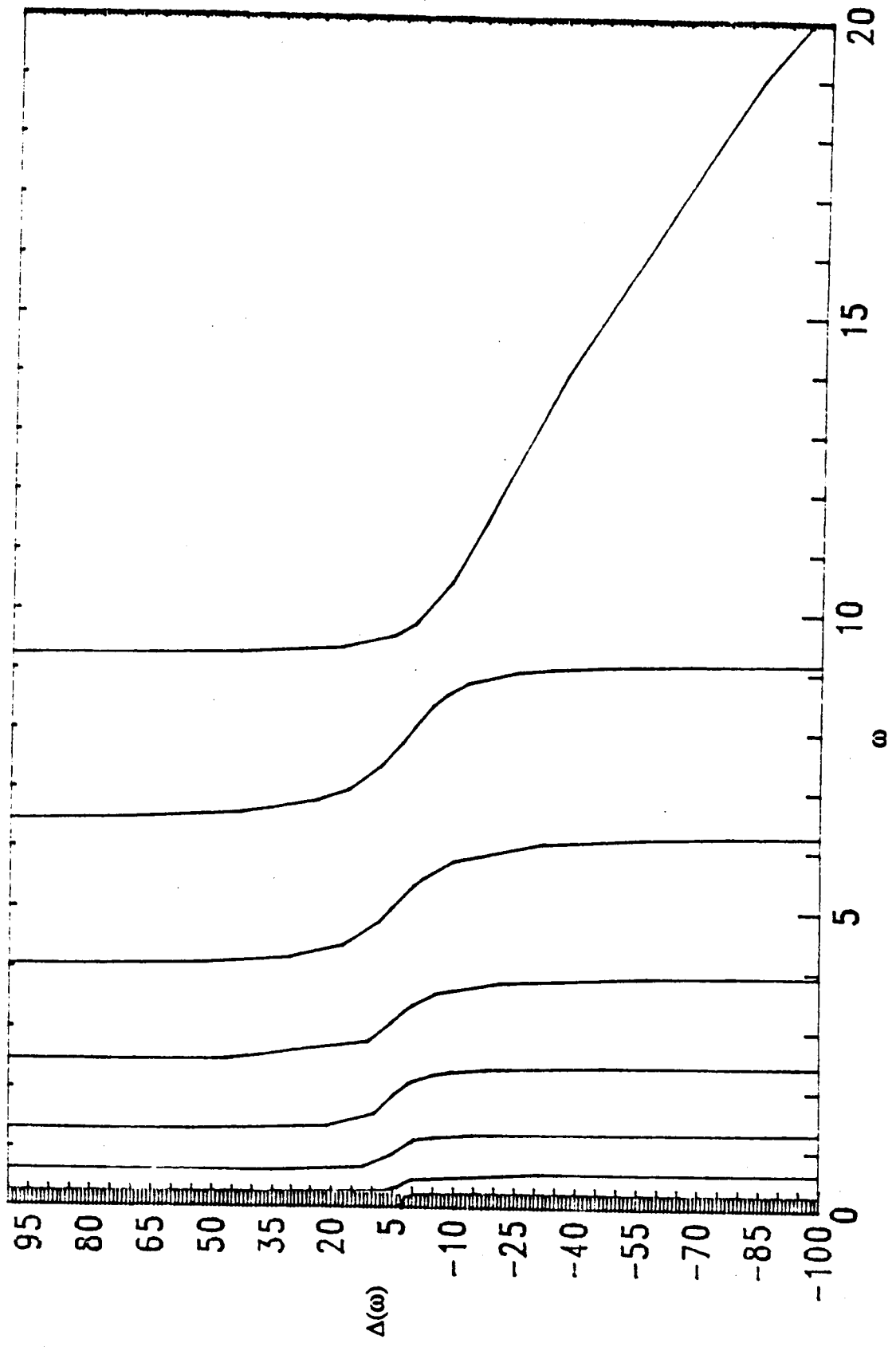


Fig 2.8 $\Delta(\omega)$ vs ω for the system of Fig 2.7

III. APPLICATION TO CONTROL DESIGN

The FETM method [13], along with its modifications [14-20], and the new method presented in Chapter II, have been developed for open loop (free vibration) analysis. A control engineer, however, is more concerned with the closed loop design and analysis, and requires an appropriate reduced model of the structure. Models consisting of finite dimensional ordinary differential equations are preferable to those consisting of partial differential equations, on the basis of practical considerations, such as the implementation of the control algorithms. Traditionally, the finite element technique is adopted to produce such models. These models, for structures with neither dissipative nor gyroscopic elements, have the form

$$M\ddot{q} + Kq = Eu \quad ; \quad q \in R^n, \quad u \in R^m \quad (3.1)$$

where the second-order state vector q consists of all the degrees of freedom, and the input vector u represents the control inputs (actuators) to the system. The symmetric mass matrix M is assumed to be positive definite, while the symmetric stiffness matrix K is assumed to be nonnegative definite.

Since n , the dimension of q , equals the total degrees of freedom, it can be very large - the larger the number of substructures that the overall structure is divided into (as is necessary to render the model of Eqn.(3.1) to be a more accurate representation of the structure), the larger is n . As a consequence, the dimension of the model hinders the straightforward applications of the existing control theories. Therefore, a need to represent the given structure by lower order models of acceptable accuracy arises.

In the field of flexible structures, the popular model reduction schemes are : the structural analysts approach [2] which retains modes corresponding to lower natural frequency; the modal cost analysis [5] which retains modes that have the largest contribution to the mission objective, measured via quadratic cost function; and the open- and closed- loop balancing method [22] which produces reduced models based on a "measure of importance" of the modes.

Note that the above model reduction methods operate at 'modal' level - i.e., they produce reduced models based on the modal data. Hence, the starting points for these methods rely upon the availability of reliable modal data. This is difficult to obtain for Eqn.(3.1), particularly when n is large - it is precisely due to this difficulty that the FETM method has been developed.

In this chapter, we show that the new method developed in Chapter II offers a procedure to aid in the control design phase. The advantages of this new method as applied to control design of flexible structures are :

- it does not require the modal data. It needs only the frequencies which , as shown in Chapter II, can be obtained *in passe*.
- it operates at the elemental/substructures level; hence, it does not require even the assembled equation (3.1).
- the reduced representation produced by this method can be tailored to suit the control architecture, such as sensor/actuator locations, centralized/decentralized feedback, output/state feedback, and mission objectives.

The properties of the resulting controllers are yet to be investigated.

3.1 Development

In order to establish that the procedure developed in Chapter II can be easily adapted for control design, we begin by considering the homogeneous version of Eqn.(3.1):

$$M \ddot{q} + K q = 0 ; \quad q \in R^n . \quad (3.2)$$

As usual, assuming a harmonic response, we get

$$S q(t) = [K - \omega^2 M] q(t) = 0, \quad (3.3a)$$

which in partitioned form, with n_1 being arbitrary, is written as

$$S_1 q_1(t) + S_{12} q_2(t) = 0, \quad q_1 \in R^{n_1} \quad (3.3b)$$

$$S_{12}^T q_1(t) + S_2 q_2(t) = 0, \quad q_2 \in R^{n_2} ; \quad n_2 \triangleq n - n_1 \quad (3.3c)$$

where

$$S_1 \triangleq K_1 - \omega^2 M_1, \quad S_2 \triangleq K_2 - \omega^2 M_2, \quad S_{12} \triangleq K_{12} - \omega^2 M_{12} . \quad (3.3d)$$

Using Eqn.(3.3b) we obtain

$$q_1(t) = -S_{1,2} q_2(t) \triangleq -S_1^{-1} S_{12} q_2(t) \quad (3.4)$$

establishing a relationship between $q_1(t)$ and $q_2(t)$. Hence, the lower part of Eqn.(3.2) yields

$$M_{2,1} \ddot{q}_2 + K_{2,1} q_2 = 0, \quad (3.5a)$$

where

$$M_{2,1} \triangleq M_2 - M_{12}^T S_{1,2} ; \quad K_{2,1} \triangleq K_2 - K_{12}^T S_{1,2} . \quad (3.5b)$$

Note that Eqn.(3.5a) is of dimension n_2 , and it still represents the original 'large' model (3.2) of dimension n with the dof q_1 "absorbed" into q_2 . Also note that the relation (3.4) and the model (3.5a) are accurate for a homogeneous system. If the system is not homogeneous, these equations are only approximate, with the degree of approximation depending on the forcing function.

Equation (3.2) represents the assembled set of equations of motion describing all the substructures, and hence is of large order, that is, n may be quite large. Since n is large, n_1 will still be large, particularly when n_2 is required to be small. If n_1 is large, then the matrix being inverted in Eqn.(3.4) is large, which may cause numerical difficulties. In order to avoid this difficulty, recall that this approach, as presented thus far, operates only on the assembled set of equations, and not at elemental level as developed in Chapter II. Therefore, we would like to develop a method that operates at elemental level - and hence, requires less computations - which would produce the same representation (3.5a). This development is given below.

Consider an i th substructure and proceed analogous to the development in Section 2.1, but involving mass and stiffness matrices in place of the dynamic stiffness matrix. This would yield, in terms of accelerations and positions, in place of Eqn.(2.9)

$$M_{r,l}^{i,i} \ddot{q}_r^i + K_{r,l}^{i,i} q_r^i = f_r^i + F_{r,l}^{i,i} f_l^i, \quad (3.6a)$$

where

$$M_{r,l}^{i,i} \triangleq M_r^i - M_n^i [S_{l,l}^{i,i}]^{-1} S_{lr}^i; \quad K_{r,l}^{i,i} \triangleq K_r^i - K_n^i [S_{l,l}^{i,i}]^{-1} S_{lr}^i, \quad (3.6b)$$

and where the superscripts and subscripts follow the same notation adopted in Eqns.(2.10a,b). Note that the matrices $M_{r,l}^{i,i}$ and $K_{r,l}^{i,i}$ are no longer symmetric, in general.

Now consider the $(i+1)$ th substructure, and suppose that there are some external (generalized) forces u^i applied along the interface of the i th and $(i+1)$ th substructures. Then the equilibrium condition (2.12) becomes

$$f_r^i + f_l^{i+1} = u^i. \quad (3.7)$$

(If there are any concentrated masses and/or spring supports that exist along the interface, they can also be accommodated as pointed out in Remark (c) of the previous chapter). Use Eqn.(3.7) and the continuity condition (2.14) to obtain the equations of motion for the interfacing dof as

$$\begin{aligned}
& [M_l^{i+1} + M_{r,l}^{i,i}] \ddot{q}_l^{i+1} + [K_l^{i+1} + K_{r,l}^{i,i}] q_l^{i+1} + M_{r,l}^{i+1} \ddot{q}_r^{i+1} + K_{r,l}^{i+1} q_r^{i+1} \\
& = F_{l,l}^{i+1,i} f_l^i + F_{l,l}^{i+1,i+1} u^i
\end{aligned} \quad (3.8)$$

Continuing again with the assumption of harmonic response, the equations of motion of the i th and $(i+1)$ th substructures assembled together, can now be written in terms of q_r^{i+1} as

$$M_{r,l}^{i+1,i} \ddot{q}_r^{i+1} + K_{r,l}^{i+1,i} q_r^{i+1} = f_r^{i+1} + F_{r,l}^{i+1,i} f_l^i + F_{r,l}^{i+1,i+1} u^i \quad (3.9a)$$

where

$$M_{r,l}^{i+1,i} \triangleq M_r^{i+1} - M_{r,l}^{i+1} [S_{l,l}^{i+1,i}]^{-1} S_{l,r}^{i+1} ; \quad K_{r,l}^{i+1,i} \triangleq K_r^{i+1} - K_{r,l}^{i+1} [S_{l,l}^{i+1,i}]^{-1} S_{l,r}^{i+1} \quad (3.9b)$$

$$F_{r,l}^{i+1,i+1} \triangleq S_{r,l}^{i+1} [S_{l,l}^{i+1,i+1}]^{-1} F_{l,l}^{i+1,i+1} .$$

Thus, the development presented thus far offers a procedure to obtain a reduced representation of the structure consisting of the i th and $(i+1)$ th substructures. If, for example, the total structure consists of only these two substructures (i.e., $N=2$, and $i=1$), and if there are applied forces u^0 along the left boundary (making $f_l^1 = u^0$), u^1 along the interface, and u^2 along the right boundary (making $f_r^2 = u^2$), then from Eqn.(3.9a), a reduced model of this structure would be

$$M_{r,l}^{2,1} \ddot{q}_r^2 + K_{r,l}^{2,1} q_r^2 = E_{r,l}^{2,1} u_{r,l}^2 , \quad (3.10a)$$

where

$$\begin{aligned}
[u_{r,l}^{2,1}]^T & \triangleq [(u^0)^T, (u^1)^T, (u^2)^T]^T \\
E_{r,l}^{2,1} & \triangleq [F_{r,l}^{2,1}, F_{r,l}^{2,2}, I]
\end{aligned} \quad (3.10b)$$

These equations can be derived directly from the results of Chapter II. This statement is verified by recognizing that

$$S_{r,l}^{i,j} = K_{r,l}^{i,j} - \omega^2 M_{r,l}^{i,j} \quad (3.11)$$

which provides the "mass" and "stiffness" matrices required of the reduced models. Moreover, from the discussions on Section 2.2.4, Variations of the Algorithm, such a reduced model can be developed in terms of any selected dof - i.e., in terms of dof either on the left boundary, or on the right boundary, or on any intermediate interfaces, or any

combination. This flexibility is required in obtaining models that are to be used for subsequent control design, since the dof we wish to keep in the reduced models will differ in general depending upon the control objectives (mission objectives) and sensor/actuator locations. We will elaborate upon this in discussions below.

It is therefore possible to produce reduced models in the form

$$M_R \ddot{q}_R + K_R q_R = E_R u \quad , \quad (3.12)$$

by employing the new method developed in Chapter II. In the representation of Eqn.(3.12), the variables q_R represent the selected degrees of freedom that were determined to be of significance by user, and u is the input vector consisting of external control forces applied on the structure.

3.2 Control Design

Having presented a means of producing reduced models, it is now in order to investigate the role of these models in control design. Toward this task, we recall Eqn.(3.1) with the control term u introduced

$$M \ddot{q} + K q = E u \quad ; \quad q \in \mathbb{R}^n, \quad u \in \mathbb{R}^m \quad , \quad (3.13a)$$

and assume that the dof to be retained have been identified as q_2 and that the entire dof vector q has been reordered so that

$$q = \begin{bmatrix} q_1 \\ q_2 \end{bmatrix} \quad ; \quad q_1 \in \mathbb{R}^{n_1} \quad ; \quad q_2 \in \mathbb{R}^{n_2} \quad (3.13b)$$

We will assume that none of the dof contained in q_1 are directly acted upon by the control forces, so that the input matrix E has the form $E^T = [0 \ E_2^T]$. With these considerations,

Eqn.(3.12) in its partitioned form is written as

$$\begin{bmatrix} M_1 & M_{12} \\ M_{12}^T & M_2 \end{bmatrix} \begin{bmatrix} \ddot{q}_1 \\ \ddot{q}_2 \end{bmatrix} + \begin{bmatrix} K_1 & K_{12} \\ K_{12}^T & K_2 \end{bmatrix} \begin{bmatrix} q_1 \\ q_2 \end{bmatrix} = \begin{bmatrix} 0 \\ E_2 \end{bmatrix} u \quad . \quad (3.13c)$$

Then the reduced model, in terms of q_2 which are relabeled now as q_R , is given by

$$M_R \ddot{q}_R + K_R q_R = E_R u \quad , \quad (3.14a)$$

where

$$\begin{aligned} M_R &\triangleq M_2 - M_{12}^T S_{1,2} \quad ; \quad K_R \triangleq K_2 - K_{12}^T S_{1,2} \quad ; \quad E_R \triangleq E_2 \\ S_{1,2} &\triangleq (K_1 - \omega^2 M_1)^{-1} (K_{12} - \omega^2 M_{12}). \end{aligned} \quad (3.14b)$$

Theorem 3.1

The reduced model (3.14) retains the frequency ω that was used to develop the model.

Proof: Assuming $u = 0$ for the evaluation of natural frequencies, Eqn.(3.14a) yields

$$\begin{aligned} \left| K_R - \omega^2 M_R \right| &= \left| K_2 - K_{12}^T S_{1,2} - \omega^2 (M_2 - M_{12}^T S_{1,2}) \right| \\ &= \left| K_2 - \omega^2 M_2 - (K_{12}^T - \omega^2 M_{12}^T) S_{1,2} \right| \\ &= \left| K_2 - \omega^2 M_2 - (K_{12}^T - \omega^2 M_{12}^T) (K_1 - \omega^2 M_1)^{-1} (K_{12} - \omega^2 M_{12}) \right| \\ &= \frac{1}{\left| K_1 - \omega^2 M_1 \right|} \left| \begin{array}{cc} K_1 - \omega^2 M_1 & K_{12} - \omega^2 M_{12} \\ K_{12}^T - \omega^2 M_{12}^T & K_2 - \omega^2 M_2 \end{array} \right| = 0 \end{aligned} \quad (3.15)$$

where Eqn.(3.14b), and the assumption that $[K_1 - \omega^2 M_1]$ is nonsingular, have been used. Observing that the second determinant of Eqn.(3.15) yields the natural frequency of the structure concludes the proof. #

An Illustrative Example.

To illustrate the use of the reduced model (3.12) in control design, we use the simply supported beam shown in Fig.3.1 of Appendix A.. It is desired to control the linear displacement (w_2) and its linear velocity at node 2, by using the linear force actuator u located at node 2. The available sensors measure the linear position and linear velocity at node 2. An output feedback control policy is desired.

For convenience of illustration, the beam is divided into two elements. Due to the statement of the problem, the w_2 dof is determined to be retained in the reduced model. Since w_2 is an intermediate dof, Eqn.(2.32c) from Variation B of the Algorithm, is used to develop the model :

$$[S_{r,l}^{1,1} + S_{l,r}^{2,2}] \begin{bmatrix} w_2 \\ \theta_2 \end{bmatrix} = \begin{bmatrix} 1 \\ 0 \end{bmatrix} u, \quad (3.16)$$

from which θ_2 can be eliminated to yield

$$S_R w_2 = u \quad (3.17)$$

By using $|S_R| = 0$, the natural frequencies of the beam are extracted. These are {0.48, 2.15, 5.32, 10.2 rad/sec.}. Once the natural frequencies are determined, a reduced model can be extracted from Eqn.(3.16) as

$$M_R(\omega) \ddot{w}_2 + K_R(\omega) w_2 = u, \quad (3.18)$$

where the argument ω is introduced to indicate that the corresponding parameters are dependent on the frequency at which S_R is computed; since there are four frequencies in this example, four reduced models can be generated.

The model (3.18) is now used for control design. Though several control design schemes can be employed at this step, we have used the Linear Quadratic Regulator (LQR) theory [23]. Since the LQR theory requires a state-space representation of the model, Eqn.(3.18) is converted to

$$\dot{x} = A x + B u, \quad (3.19)$$

$$x \triangleq \begin{bmatrix} w_2 \\ \dot{w}_2 \end{bmatrix}, \quad A \triangleq \begin{bmatrix} 0 & I \\ -M_R^{-1} K_R & 0 \end{bmatrix}, \quad B \triangleq \begin{bmatrix} 0 \\ 1 \end{bmatrix}.$$

Then the application of LQR theory yields the feedback control

$$u = -g^T x = -g_1 w_2 - g_2 \dot{w}_2 \quad (3.20)$$

that minimizes

$$J = \int_0^{\infty} \{ w_2^2(t) + \dot{w}_2^2(t) + \rho u^2(t) \} dt, \quad (3.21)$$

subject to (3.19), where ρ is a design parameter, variation of which produces different gains $\{g_1, g_2\}$ and hence, controllers of different bandwidth. Note that the control policy of Eqn.(3.20) can be implemented as an output feedback on the beam, since w_2 and \dot{w}_2 are available as sensor signals.

Note that this design methodology does yield an output feedback control policy as required, and it has been developed by minimizing the objective function J of Eqn.(3.21) which represents the suppression of position and velocity at node 2. However, this policy has been designed based upon the approximation (3.18), and not based upon the true representation of the beam. Hence, in order to evaluate the performance of this control, it is

compared with the performance of the control that is designed based upon the true representation of the beam - a fourth order finite element model involving all the dof $\{\theta_1, w_2, \theta_2, \theta_3\}$ has been used as a true model. The comparison is shown in Fig.3.2 of Appendix A.

In Fig.3.2 of Appendix A, the labels 'regulation cost' and 'control cost' are defined as follows:

$$\begin{aligned} \text{control cost} &\triangleq \int_0^{\infty} u^2(t) dt \\ \text{regulation cost} &\triangleq \int_0^{\infty} \{ w_2^2(t) + \dot{w}_2^2(t) \} dt \end{aligned} \quad (3.22)$$

for some assumed initial conditions. Each value of ρ in (3.21) produces a point; each curve is produced by varying ρ and by calculating the control cost and regulation cost. The 'optimal' curve in this figure represents the performance of the system while using the control designed based upon the true model; the 'performance curve' corresponding to those controls that were developed based upon the approximation (3.18) would therefore be above the optimal curve. Since each natural frequency yields a different approximation (3.18), there are four performance curves in Fig.3.2 of Appendix A, each corresponding to one natural frequency.

Observe that the approximation (3.18) obtained with $\omega = \omega_1$ yields the best suboptimal controllers, indicating that the lowest natural frequency is the most significant mode in this control problem. This is to be expected since the first mode has the maximum effect on w_2 (the dof we wish to control) and on the sensors, and is affected the most by the actuator. Similarly the $\omega = \omega_4$ curve indicates that the highest mode is the least significant. Notice that the performance difference between the optimal curve and the $\omega = \omega_1$ curve is only marginal. The controllers from the controllers from $\omega = \omega_1$ curve are implementable as output feedback, while the optimal controllers (those from the optimal curve) are not implementable since they require feedback of the positions and velocities of all the dof, which in this example are not directly available. Therefore with $\omega = \omega_1$, the approximation (3.18) produces fairly acceptable feedback designs.

Another observation from this figure is that the closed loop system employing the suboptimal controllers remains asymptotically stable for all control cost. This is normally not expected of suboptimal controllers since the effect of errors in the approximation (3.18) is to drive the closed loop system unstable while using large feedback gains; see Ref.[24] for discussions on effect of model errors. This unexpected observation is explained by the following theorem.

Theorem 3.2

For a single input system, independent of the order of the full model (3.12), the feedback control designed employing the LQR theory based upon the approximation (3.14) is guaranteed to yield the closed loop system atleast marginally stable, if the approximation is a scalar equation (i.e., $n_2=1$).

The proof relies upon the following Lemma.

Lemma 3.1

The gains g_1 and g_2 involved in the control law

$$u = -g_1 x - g_2 \dot{x} \quad (3.23a)$$

that minimizes

$$\int_0^{\infty} \{ q_1 x^2 + q_2 \dot{x}^2 + \rho u^2 \} dt \quad (3.23b)$$

subject to

$$m\ddot{x} + kx = eu, \quad (3.23c)$$

where $m > 0$, $k > 0$, q_1 , q_2 , and ρ are arbitrary positive scalars, satisfy

$$eg_1 > 0, \quad eg_2 > 0. \quad (3.24)$$

Proof :

Convert the minimization problem into the standard linear quadratic regulator problem as

$$\min \int_0^{\infty} \{ [x \ \dot{x}]^T \begin{bmatrix} q_1 & 0 \\ 0 & q_2 \end{bmatrix} \begin{bmatrix} x \\ \dot{x} \end{bmatrix} + \rho u^2 \} dt \quad (3.25a)$$

subject to

$$\begin{bmatrix} \dot{x} \\ \ddot{x} \end{bmatrix} = \begin{bmatrix} 0 & 1 \\ \frac{k}{m} & 0 \end{bmatrix} \begin{bmatrix} x \\ \dot{x} \end{bmatrix} + \begin{bmatrix} 0 \\ \frac{e}{m} \end{bmatrix} u \quad (3.25b)$$

The solution to this problem is the full state feedback control [23]

$$u = -\frac{1}{\rho} \begin{bmatrix} 0 & \frac{e}{m} \end{bmatrix} \begin{bmatrix} k_{11} & k_{12} \\ k_{12} & k_{22} \end{bmatrix} \begin{bmatrix} x \\ \dot{x} \end{bmatrix} = -\frac{1}{\rho} \begin{bmatrix} \frac{e}{m} k_{12} & \frac{e}{m} k_{22} \end{bmatrix}, \quad (3.25c)$$

where the k_{ij} ($i,j = 1,2$) satisfy the Riccati equation

$$\begin{aligned}
& \begin{bmatrix} k_{11} & k_{12} \\ k_{12} & k_{22} \end{bmatrix} \begin{bmatrix} 0 & 1 \\ \frac{k}{m} & 0 \end{bmatrix} + \begin{bmatrix} 0 & \frac{k}{m} \\ 1 & 0 \end{bmatrix} \begin{bmatrix} k_{11} & k_{12} \\ k_{12} & k_{22} \end{bmatrix} + \begin{bmatrix} q_1 & 0 \\ 0 & q_2 \end{bmatrix} \\
& - \begin{bmatrix} k_{11} & k_{12} \\ k_{12} & k_{22} \end{bmatrix} \begin{bmatrix} 0 \\ \frac{e}{m} \end{bmatrix} \frac{1}{\rho} \begin{bmatrix} 0 & \frac{e}{m} \end{bmatrix} \begin{bmatrix} k_{11} & k_{12} \\ k_{12} & k_{22} \end{bmatrix} = 0.
\end{aligned} \tag{3.25d}$$

Comparing Equations (3.25c) and (3.23a) reveals that

$$eg_1 = \frac{e^2}{\rho} k_{12}, \quad eg_2 = \frac{e^2}{\rho} k_{22}. \tag{3.26}$$

Therefore, to prove Lemma 3.1, we need to show that $k_{22} > 0$, and $k_{12} > 0$.

Now, since q_1 and q_2 are positive, it follows from the positive definite property of the Riccati solution [23] that

$$k_{22} > 0, \quad k_{11} > 0, \quad k_{11}k_{22} - k_{12}^2 > 0. \tag{3.27}$$

Hence, $eg_2 > 0$, as claimed in the lemma. To show that $k_{12} > 0$, rewrite Eqn.(3.25d) in its partitioned form as

$$-2\frac{k}{m}k_{12} + q_1 - \frac{1}{\rho m^2}k_{12}^2 = 0, \tag{3.28a}$$

$$k_{11} - \frac{k}{m}k_{22} - \frac{1}{\rho m^2}k_{12}k_{22} = 0, \tag{3.28b}$$

$$2k_{12} - \frac{1}{\rho m^2}k_{22}^2 + q_2 = 0. \tag{3.28c}$$

Solve for k_{12} from Eqn.(3.28a) to get

$$\frac{2k_{12}}{\rho m} = \left\{ -k + \sqrt{k^2 + \frac{1}{\rho}} \right\} \quad \text{or} \quad \left\{ -k - \sqrt{k^2 + \frac{1}{\rho}} \right\}. \tag{3.29a}$$

Substituting the above result in Eqn.(3.28b) yields

$$k_{11} = \frac{k_{22}}{m} \sqrt{k^2 + \frac{1}{\rho}} \quad \text{or} \quad -\frac{k_{22}}{m} \sqrt{k^2 + \frac{1}{\rho}}. \tag{3.29b}$$

Now, since k_{11} must be positive, the correct solution for k_{12} is

$$\frac{2k_{12}}{\rho m} = -k + \sqrt{k^2 + \frac{1}{\rho}} > 0. \quad (3.29c)$$

Hence, $eg_1 > 0$. #

Proof of Theorem 3.2:

Since the approximation (3.14) is a scalar equation, it follows from Lemma 3.1 that the feedback gains in the resulting control policy

$$u = -g_1 q_R - g_2 \dot{q}_R \quad (3.30)$$

satisfy $E_R g_1 > 0$, and $E_R g_2 > 0$.

Now, since $q_R = q_2$ and $E_R = E_2$, the control law (3.30), when implemented in the overall system of Eqn.(3.13c) renders the closed loop system as

$$M_c \ddot{q} + D_c \dot{q} + K_c q = 0, \quad (3.31a)$$

where

$$M_c \triangleq M = \begin{bmatrix} M_1 & M_{12} \\ M_{12}^T & M_2 \end{bmatrix} > 0 \quad (3.31b)_1$$

$$D_c \triangleq \begin{bmatrix} 0 & 0 \\ 0 & E_2 g_2 \end{bmatrix}, \quad K_c \triangleq \begin{bmatrix} K_1 & K_{12} \\ K_{12}^T & K_2 + E_2 g_1 \end{bmatrix} \quad (3.31b)$$

Now, since $E_2 g_2$ and $E_2 g_1$ are positive scalars, and since

$$K_c = K + \begin{bmatrix} 0 & 0 \\ 0 & E_2 g_1 \end{bmatrix}, \quad (3.32)$$

we get $D_c \geq 0$, $K_c > 0$ (since $K > 0$). Therefore, from the properties of mechanical systems[25], the system of Eqn.(3.31) is atleast marginally stable. #

In conclusion of this Section, we point out that only a preliminary study of the applicability of the proposed method to control design has been presented. A more detailed study is in progress. The example included herein has served to illustrate the output feedback design using the new method. The results are satisfactory. An issue raised by this example is the following: Since each natural frequency yields a n approximation, one could conceivably obtain many approximations; as many as the total number of frequencies of the system. Hence, the development of the performance plot (as in Fig. 2 of Appendix A) including all of these approximations would be time consuming. This burden may be

reduced if the "significant" frequencies (such as the first frequency in the example) can be determined *a priori* - one might adopt the modal cost analysis of Ref.[5] for this task.

The application of this method to a decentralized control design is given in Appendix B.

IV. CONCLUSIONS AND RECOMMENDATIONS FOR FUTURE RESEARCH

The objective of this research effort was to develop a methodology that unifies the modeling problem and the control design problem. There exist a few methods in structural analysis and control design that may be integrated to produce such a unifying scheme. We have investigated the adaptability of the finite-element transfer-matrix (FETM) approach for this task. Specifically, we have developed a new method to overcome the limitations of the FETM method. This new method is capable of producing reduced models of structures, that can be tailored to suit the control design phase. The applicability of this method to controller design - both output feedback and decentralized control - has been illustrated through an example.

The progress of this research has raised several issues that need to be addressed in future:

1. The new method requires an efficient numerical scheme for updating the assumed frequencies during the extraction of the structural natural frequencies. An appropriate scheme needs to be selected or developed.
2. The approximations produced by the new method, though yielding acceptable controllers, do not preserve the symmetric properties of the original structure. The role of these approximations as reduced models is questionable. An appropriate modification of this method is hence required. This modification is near completion and requires further investigation.
3. Since the reduced model depends upon the frequency using which it has been derived, each natural frequency yields a different reduced model, and one could conceivably obtain many reduced models. This raises the question of which one (or which few) of the natural frequencies are to be used for the generation of the reduced models. In order to answer this question one needs to determine *a priori* the 'significant' frequencies, such as those identified by modal cost analysis, for example. This issue has to be resolved for the proposed method to be a feasible controller design scheme.
4. The controller design based upon the proposed method needs to be explored further. We believe that, since the reduced model is directly related to the full model, in terms of frequency, and the mass and stiffness matrices, the performance of the controller with respect to the full model could be predicted. In particular, the

stability of the overall closed loop system could be predicted, as established by Theorem 3.2 in a special case. The stability properties of matrix second order systems would naturally be used here.

5. An important requirement of any control design is the robustness of the controller. This issue needs to be addresses in the future.

REFERENCES

1. A. Yousuff, "Model Errors - Should They Always be Minimized?," *IEEE Mid-West Symp. on Circuits and Systems*, Louisville, KY, Aug.19-20, 1985.
2. L. Meirovitch, H.Öz, "An Assessment of Methods for the Control of Large Space Structures," in *Proc. 1979 JACC*, pp.34-41.
3. R.E. Skelton, C.Z.Gregory, "Measurement Feedback and Model Reduction by Modal Cost Analysis," in *Proc. 1979 JACC*, pp.211-218.
4. R.E. Skelton, "Large Space System Control Technology: Model Order Reduction Study," *Large Space System Technology*, 1979, NASA CR-2118, pp.313-321.
5. R.E. Skelton, P.C. Hughes, "Modal Cost Analysis for Linear Matrix Second Order Systems," *J. Dyn. Sys. Meas. Control*, Vol.102, Sep. 1980.
6. W. A. Stauffer, R.L. Ross, J. G. Lewolt, "Fuel Conservative Subsonic Transport," *Active Controls in Aircraft Design*, AGARD-AG-234, 1978, pp.9.1-9.13.
7. "Control/Structure Interaction in Flexible Space Structure," in *Amer. Control Conf.*, Boston, MA, June 19-21, 1985.
8. "Control/Structure Interaction in Flexible Space Structure," in *IEEE Conf. Dec. Control*, Fort Lauderdale, FL, Dec.11-13, 1985.
9. *NASA/DoD Control/Structure Interaction Technology 1986*, NASA Conference Publication 2447, Part 1., Norfolk, VA, Nov. 18-21, 1986.
10. V. B. Venkayya, V. A. Tischler, "Frequency Control and Its Effect on the Dynamic Response of Flexible Structures," *AIAA Journal*, Vol.23, No.11, Nov.1985, pp.1768-1774.
11. L. Meirovitch, Editor, *Dynamics and Control of Large Structures*, 4th VPI & SU/AIAA Symp., Blacksburg, VA, June 1983.
12. A. K. Noor, S. N. Atluri, "Advances and Trends in Computational Structural Mechanics," *AIAA Journal*, Vol.25, No.7, July 1987, pp.977-995.
13. M. A. Dokainish, "A New Approach for Plate Vibrations: Combination of Transfer Matrix and Finite-Element Technique," *J. Eng. Ind. Trans. ASME*, Series B94, 1982, pp.526-530.
14. G. Chiatti, A. Sestieri, "Analysis of Static and Dynamic Problems by a Combined Finite Element-Transfer Matrix Method," *J. Sound Vib.*, Vol.67, 1979, pp.35-42.
15. V. H. Mucino, V. Pavelic, "An Exact Condensation Procedure for Chain-Like Structures Using a Finite Element-Transfer Matrix Approach," *J. Mech. Design*, V103, 1981, pp.296-303.

16. T. J. McDonald, K. B. Eversole, "A Combined Finite Element-Transfer Matrix Structureal Analysis Method," *J. Sound Vib.*, Vol.51, 1977, pp.157-169.
17. S. Sankar, S. V. Hoa, "An Extended Transfer Matrix-Finite Element Method for Free Vibration of Plates," *J. Sound Vib.*, Vol.70, 1980, pp.205-211.
18. M. Ohga, T. Shigematsu, T. Hara, "Structural Analysis by a Combined Finite Element-Transfer Matrix Method," *Comput. Struct.*, Vol.17, 1983, pp.321-326.
19. E. C. Pestel, "Note: Rectangular Transfer Matrices," *Int. J. Mech. Sci.*, Vol.5, 1983, pp.419-421.
20. E. Degen, M. Shephard, R. Lowey, "Combined Finite Element-Transfer Matrix Method Based on Mixed Formulation," *Comput. Struct.*, Vol.20, 1985, pp.173-180.
21. E. C. Pestel, F. A. Leckie, *Matrix Methods in Elastomechanics*, McGraw-Hill, New York, 1963.
22. E. A. Jonckheere, Ph. Opdenacker, "Singular Value Analysis, Balancing, and Model Reduction of Large Space Structures," in *Proc. Amer. Control Conf.*, San Diego, CA, June 1984, pp.141-149.
23. H. Kwakernaak, R. Sivan, *Linear Optimal Control Systems*, John Wiley & Sons, Inc., New York, NY, 1972.
24. R. E. Skelton, "Control Design of FLexible Spacecraft," *Theory and Appl. of Opt. Control in Aerospace Systems*, Ed. P. Krant, Netherlands, 1981.
25. K. Magnus, "Der Einfluss vershiedener Kräftearten auf die Stabilität Lineares Systeme," *Z. Agnew, Math. Phys.*, Vol.21, No.4, 1970, pp.523-534.

APPENDIX A.

Control of Flexible Structures by Finite Element-Transfer Matrix Approach

**IFAC Symposium on Control of Distributed Parameter Systems,
Los Angeles, CA, June 30 - July 03, 1986.**